Eurographics/ IEEE-VGTC Symposium on Visualization 2008
A. Vilanova, A. Telea, G. Scheuermann, and T. Möller
(Guest Editors)

Volume 27 (2008), Number 3

Interactive Visualization of Multimodal Volume Data for Neurosurgical Tumor Treatment

Christian Rieder[1,2], Felix Ritter[1], Matthias Raspe[2], and Heinz-Otto Peitgen[1]

[1]MeVis Research GmbH, Center for Medical Image Computing, Bremen, Germany
[2]Computer Graphics Working Group, University of Koblenz-Landau, Germany

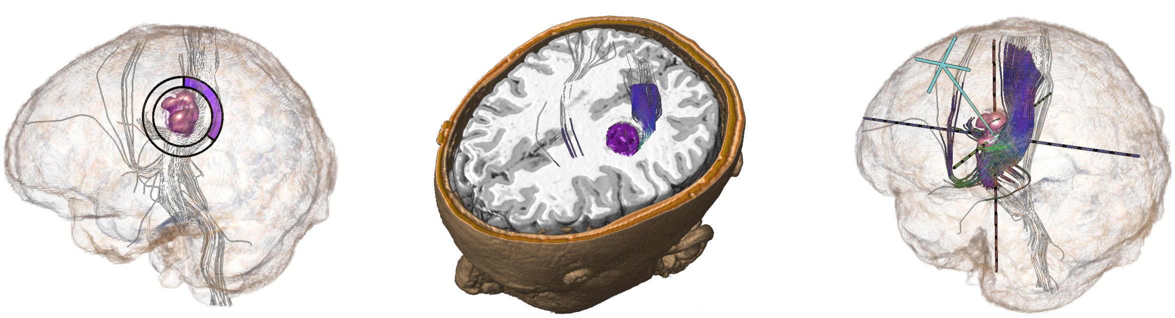

Teaser Figure: *Left: Brain, visualized using silhouettes, the lesion's spatial depth is displayed using a ring. Center: Combined rendering of brain tissue, skull and fiber tracts using a cutting plane. Right: The virtual path (cyan) from the entry point to the region of interest. The two crossed lines represent the diameter of the virtual cylinder.*

Abstract

We present novel interactive methods for the visualization of multimodal volume data as used in neurosurgical therapy planning. These methods allow surgeons to explore multimodal volumes and focus on functional data and lesions. Computer graphics techniques are proposed to create expressive visualizations at interactive frame rates to reduce time-consuming and complex interaction with the medical data. Contributions of our work are the distance-based enhancements of functional data and lesions which allows the surgeon to perceive functional and anatomical structures at once and relate them directly to the intervention. In addition we propose methods for the visual exploration of the path to the structures of interest, to enhance anatomical landmarks, and to provide additional depth indicators. These techniques have been integrated in a visualization prototype that provides interaction capabilities for finding the optimal therapeutic strategy for the neurosurgeon.

Categories and Subject Descriptors (according to ACM CCS): J.3 [Life And Medical Sciences]: Health; I.4.10 [Image Presentation]: Volumetric;

1. Introduction

The brain is one of the vital parts of the human body. However, essential functionality such as motor activity or speech can be derogated by pathological tissue, e.g. tumors. Depending on the severity of the damage, neurosurgery is necessary to treat the lesion. Planning such a neurosurgery involves multimodal data of different protocols and parametrizations to identify functional areas and find the optimal access path to the lesion. The goal of neurosurgery planning is to find an access path to the lesion while minimizing the damage to vital and healthy tissue. In order to achieve this, functional data such as functional magnetic resonance imaging data (fMRI: for detection of activation areas) or diffusion tensor imaging data (DTI: for reconstruction of fibers) has to be combined with anatomical data from MRT or CT devices. Usually, the surgeon analyzes the available data on a slice-by-slice basis, while mentally merging the multimodal images in three dimensions. The visualization of multimodal data in a combined form would improve recognition and the knowledge of where risk structures are located.

In our neurosurgical prototype, we carefully combine recent visualization methods and add new visualization techniques that were requested by medical experts to facilitate the exploration of multimodal volume data. The value of this paper lies in the structure that we present for the development of effective multimodal neurosurgical planning systems. With regard to neurosurgeons, whose traditional field of work is not computer science, we chose techniques that enable the visualization of medical data with minor interaction requirements and that facilitate the fast recognition of structures of interest. Particularly, the therapeutic strategy strongly depends on the visualization of risk structures as well as anatomical details along the trajectory. We show in this article in which directions future surgical planning applications might emerge to achieve high acceptance in the neurosurgical domain. The technical contributions of our paper are:

- *Distance-based combination of transfer functions for lesion accentuation.* By enhancing the rendering of pathological structures we are able to attenuate anatomical details that are far away from the lesion. Particularly, contrast enhanced tumors can be emphasized without the need of a segmentation mask.
- *Distance-based enhancement of functional data.* The idea is to show only functional data located close to structures of interest because structures far away from the lesion are of less importance for surgery planning. We propose the reduction of the saturation for MRI data and outline distant fiber tracts.
- *Increasing depth perception.* We introduce the distance ring which indicates the location of a structure in view direction and add a three-dimensional coordinate system. These techniques are combined with distance color blending to improve the perception of spatial depth of anatomical and functional structures.
- *Defining superficial landmarks.* We add a three-dimensional coordinate system to trace back the lesion in opaque volume rendering. An intuitive mechanism to remove the skull enables the user to examine the brain's anatomy. These tools simplify the recognition of landmarks which can be transferred into the operation site.
- *Visualization of the access path.* The use of a virtual access path in our application enables the surgeon to determine an optimal incision point fast and easily without the need of traditional cutting tools. The proposed technique enables the combined rendering of anatomical and functional data along the trajectory.

2. Related Work

2.1. Multimodal Volume Data for Visualization

Rößler et al. [RTF*06] describe a GPU-based multi-volume framework for the visualization of functional brain images. The framework uses the graphics hardware for interactive visual exploration of the data and for generating of high-quality visual representation. We extend the proposed solutions for overlapping multiple volumes in our work. Wilson et al. [WLM02] show that the visualization of multimodal volumes can help to improve the understanding of volumetric medical data. The use of illustrative techniques [BG05] in addition to transparency in multi-volume visualization provides information which is not available in single, traditional volume rendering. In this framework, different rendering styles can be applied for each volume which is also the basis of our framework. Cutting-tools are powerful and general utilities for the visualization of multimodal volume data [MFOF02]. In their paper, Manssour et al. verify that cutting tools can reveal additional diagnostic information. In our work, one key feature is a geometric cutting tool which allows to explore a virtual access path.

2.2. Enhancement of Medical Structures

Bruckner et al. [BGK06] and Viola et al. [VFSG06] propose alternatives to geometric clipping techniques for volume visualization. The developed techniques allow for perceiving context information by exploring the interior of a data set without requiring prior segmentation. Because we are using a segmented brain volume we are able to simplify the adjustment of parameters for the visual exploration. Ebert et al. [ER00] introduce the concept of volume illustration and describe illustration motifs in [SES05]. In their works methods for feature, depth and orientation enhancement are presented. In our application we leverage the techniques boundary enhancement, silhouettes [CMH*01] and distance color blending. Tappenbeck et al. [TPD06] present distance as a second dimension for transfer function definition. They compute a distance volume by slice-based selection of distance ranges. We compute the distance from a single point to every voxel as proposed in [ZDT04]. Additionally, the distance from every voxel to a given line is computed in order to enhance medical structures along a trajectory.

2.3. Computer Assisted Neurosurgical Planning

Beyer et al. [BHWB07] introduce an application for neurosurgical planning with high-quality interactive multimodal volume rendering. They use raycasting for multi-volume rendering and describe the required data and memory management. Skull peeling is presented as an extension of the opacity peeling algorithm introduced by Rezk-Salama et al. [RSK06] using registered CT and MRT data. In our work, we do not rely on CT data and use the information of MRT, fMRT and DTI data. Thus, the opacity peeling algorithm would not be straightforward to use due to the difficult adjustment of parameters. Also, we base the discussions of our methods and their combination as well as their parameterization on the medical requirements. Köhn et al. [KWK*07] present an application with integrated tools for functional data analysis together with automatic skull stripping, vessel extraction and manual segmentation of lesions or risk structures. In our work, we use this application for medical data analysis, registration, and segmentation.

3. Visualization of Multimodal Volume Data

Typical medical applications for multimodal neurosurgical planning display the medical data in a single viewport. Because functional data such as fMRI or DTI data are located in the brain itself, these data cannot be explored simultaneously with anatomical data. Therefore, physicians have to use cutting tools to explore the volume. The problem with using cutting tools is the high degree of interaction that is typically required. Also, the advantage over MPR (Multi Planar Reformatting) views is small, because in both views the visualization of functional and anatomical data is difficult due to occlusion issues and has to be integrated mentally, slice-by-slice.

3.1. Dual Views for internal and external Volume Data

In our work we present dual views for visualizing multimodal volume data. The internal view (see Figure 7 (a)) is a general view of all internal data such as fMRI activation volumes, DTI fiber tracts and the lesion, which are actually hidden by the brain and the skull. For this purpose, we choose a transfer function which hides the skull and reduces the brain to contours. Now all functional data as well as lesions can be displayed without using any cutting tools.

Since functional data are related to anatomical regions and anatomical structures are almost hidden in the first view, we use a second viewport to visualize the brain and the skull opaque, as well as the functional data. In this viewport, the anatomical details are rendered using volume lightingand boundary enhancement [ER00] to get a better three-dimensional perception (see Figure 7 (b)). The functional data must still be visualized by using cutting tools because the brain and skull occlude the brain tissue (see Teaser Figure (middle)). These two views are coherent. Every point in the internal view has a corresponding point in the external view.

The connection between the two viewports and the usage of our cutting tools are discussed in Section 4.

3.2. Distance-based Combining of Transfer Functions for Lesion Enhancement

In our application we integrated MPR views (see Figure 7), too, because most physicians are used to work with this kind of view. In the MPR views, a point of interest $\boldsymbol{p}_{ROI}$ can be specified by clicking, e.g. at the lesion. The radius r_{ROI} defines the spherical region of interest (ROI). We combined a transfer function for visualizing opaque lesion structures with a transfer function for visualizing transparent anatomy to a two-dimensional transfer function [KKH02]. We perform the computation of the distance d_{voxel} from every voxel $\boldsymbol{p}_{voxel}$ to the ROI on the graphics hardware. The distance is used to specify the second dimension of the two-dimensional transfer function.

The maximum distance value r_{ROI} as well as the transfer function's opacities and colors can be specified by the user. The Teaser Figure (left) shows that the tumor is rendered opaque and the tissue of the brain transparent, (middle) shows the opaque rendering of the brain tissue and the clipped skull.

3.3. Distance-based Enhancement of Functional Data

3.3.1. Enhancement of fMRI data

There are some issues using fMRI activation volumes, however. First, a plausible color coding is challenging. Traditionally, positive fMRI activation areas are colored red and the negative green. Also, most applications use red as a signal color for lesions like tumors. Thus, red structures can be mixed up easily, because of the same color and similar structure. Second, some of the activation areas are unimportant for the diagnosis and only cause a more complex visualization. Both problems are displayed in Figure 1 (a), where the functional data can easily be mistaken for the lesion.

Thus, in our prototype we use the color purple for lesions to be distinguished from fMRI data. Also, we fade out the color's saturation of the fMRI structures depending on the distance d_{fMRI} to the ROI by computing the length from every voxel to the ROI using a shader program (see Figure 1).

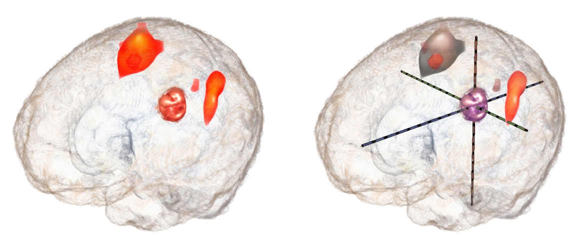

(a) (b)

Figure 1: *In (a) the tumor is colored red, as the fMRI data (without color blending $d_{fMRI} = max$), in (b) the tumor is colored purple whereas the saturation of the fMRI data is reduced ($d_{fMRI} = 15$).*

3.3.2. Enhancement of DTI data

White matter DTI data are mostly visualized as fiber tracts [VZKL05] for neurosurgical intervention planning. To create fiber tracts the user has to define a ROI from which the fiber tracking algorithm starts the reconstruction. After this reconstruction, the user has few possibilities in reducing unimportant fibers that are far away from the ROI, which can increase the complexity of the visualization (see Figure 2 (a)). Techniques, such as fiber bundle selection [BBP*05], allow to enhance fiber bundles but do not enable the attenuation of fiber bundles far away from the ROI.

We chose a similar strategy as in the fMRI data enhancement to hide fibers, which are not important for diagnosis. By defining a maximum distance d_{DTI} around the ROI, we change the representation method for fibers with a distance larger than the maximum. These fibers are just visualized as outlined silhouettes (see Figure 2 (b)) using a shader program. This is an easy and fast method to show only the diagnostically relevant DTI data, because less interaction is required. Furthermore, our technique can easily be combined with techniques such as fiber bundle selection as well as fiber clustering [OW07].

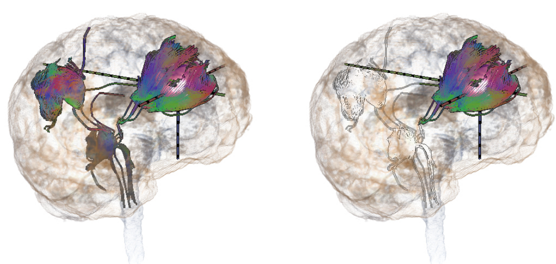

(a) (b)

Figure 2: *(a) Brain with reconstructed fiber tracts, displayed entirely ($d_{DTI} = max$); (b) reduced to silhouettes in dependence ($d_{DTI} = 31$) of the distance to the ROI (b).*

3.4. Depth Perception

In the internal view, we observed some difficulties with correctly perceiving spatial depth. By visualizing the brain as contours, the user loses the perception of depth which can yield a difficult association of the functional data with its anatomic region.

3.4.1. Distance Color Blending

By using a color gradient from a warm color in the front to a cool color in the back of the volume, the spatial depth can be intensified. The computation is done in a fragment shader where the front voxel of the volume is assigned the warm color and the back voxel the cold color in view direction, respectively. The color values between back and front are computed using linear interpolation. We use this technique in the internal views (Figures 1–3) to visualize the brain.

3.4.2. Three-Dimensional Coordinate System

The distance color blending alone does not allow for perceiving an optimal spatial depth. Therefore, we added a three-dimensional coordinate system to the internal view. The center of the coordinate system is defined as the center point of the clicked ROI. The axes run parallel to the three main directions of the volume data and end at the hull of the brain. If the head of the patient is not properly aligned, the coordinate system has to be justified manually. An algorithm performs a texture lookup into the mask volume of the brain. If the position is inside the brain, the axes will be displayed, if outside, the axes will be hidden.

In combination with the distance color blending, the perception of the spatial depth is improved. Figures 2–3 show the three-dimensional coordinate system. In comparison to Figure 1 (a) the spatial localization of the tumor is facilitated by the displayed coordinate system (Figure 1 (b)).

3.4.3. Distance Ring

At some orientations, however, the perception of the spatial depth becomes difficult because one of the axes could be hidden by other structures or because of the perspective distortion. For example, in Figure 3 (a) the axis in view direction is not visible. It is difficult to decide if the tumor is more at the front or at the back side of the volume.

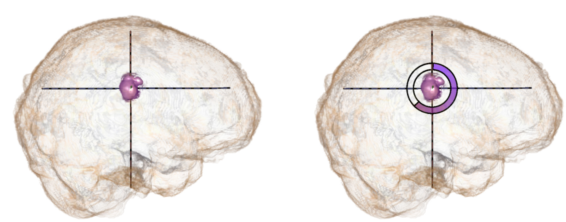

(a) (b)

Figure 3: *(a) If one of the axes is not visible, the perception of the spatial depth is difficult. (b) The ring is more than half closed ($d_{ring} = 0.64$), so the ROI is near the center of the brain at the back side in view direction*

To solve this issue, we propose an additional visualization aid to further intensify spatial information. We introduce an instrument called the distance ring. The distance ring is a simple ring which indicates the location of the ROI in the view direction. At minimal distance $d_{ring} = min$ in view direction, i.e. the ROI is at the nearest point inside the brain, the distance ring is completely open. If the distance $d_{ring} = max$, the distance ring is completely closed. The ring closes clockwise between $d_{ring} = min$ and $d_{ring} = max$. Figure 4 illustrates the computation of the distance ring.

The computation is performed in a fragment shader by tracing two rays through the brain mask volume (from ROI to back and from ROI to front): while intensity > 0:

$$\boldsymbol{p}_{test_{i+1}} = \boldsymbol{p}_{test_i} + (\boldsymbol{v}_{ray} c_{step})$$
$$c_{front_{i+1}} = c_{front_i} + c_{step}$$

where $\boldsymbol{p}_{test}$ is the position to be tested, $\boldsymbol{v}_{ray}$ is the view direction, c_{step} is the current step size and c_{front} is the amount of

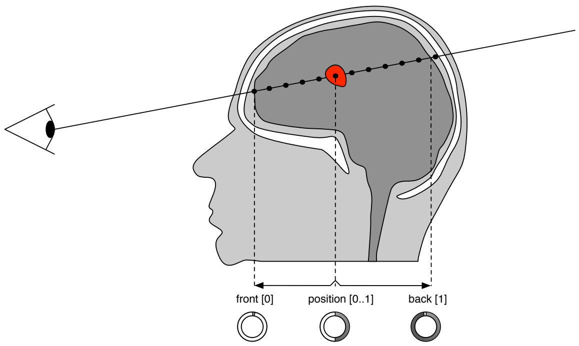

Figure 4: *Computation of the distance ring. Two rays are traced through the volume from the ROI to the backside and frontside along the view direction. The steps are counted to compute the distance of the ROI.*

steps to the front side of the brain. The computation of c_{back} is analogous.

The normalized distance d_{ring} of the ROI is the inverse of the maximum distance $c_{front} + c_{back}$ multiplied with the amount of steps of the front ray c_{front}:

$$d_{ring[0..1]} = (c_{front} + c_{back})^{-1} c_{front}$$

With the value d_{ring} we compute the closed ring in a second shader. A value of 0.0 means the ring is completely open, a value of 1.0 means the ring is closed and values between 0.0 and 1.0 close the ring clockwise from 0 to 360 degrees (see Figure 3 (b)).

4. Virtual Intervention Planning

In Section 3.1 we described the dual views, the internal view and the external view. The methods and visualizations we propose in the following sections are for internal views only. These visualizations allow to explore functional data as well as lesions which often cannot be distinguished from other tissue. While the neurosurgeon can explore the functional data during planning, he cannot utilize this information during the intervention, as no visual landmarks can be derived from the anatomy at the operating field. For this reason, we introduce the second view, the external view.

4.1. Defining Superficial Landmarks

In the external view we are able to connect functional data and lesions with anatomic cerebral structures such as gyri and sulci (ridges and fissures in the brain's surface). To support navigation, we added a three-dimensional coordinate system to the external view as well. By evaluating the exit points of the axes and repainting the points onto the patients skull before surgery, the neurosurgeon is able to mentally reconstruct the invisible ROI during surgery.

4.2. Visualization of Path to Structure of Interest

In general, neurosurgical interventions are performed using an operation microscope. Because the operation microscope and the operation field have to be in line, we propose a virtual access simulation – the virtual path – which can be interactively modified by the user. The virtual path is a simple cylinder geometry from the incision point to the ROI. Since functional data far away from the path are of minor interest, we extend the distance-based enhancement of functional data (discussed in Section 3.3). Therefore, we additionally attenuate functional data depending on the distance from every voxel to the trajectory. Thus, the neurosurgeon is able to explore the optimal path to the structure of interest.

4.2.1. Path in the Internal View

In the internal view, the path is visualized as a thin line from the incision point to the target of the surgery. At the incision point there are two orthogonal lines which define the diameter of the virtual cylindric path. Therefore, it is possible to search a path which avoids contact with functional structures like fMRI activation areas.

The internal view gives an overview of all internal data but not the precise location of the anatomical region. The Teaser Figure (right) shows the virtual path (cyan) from an entry point to the ROI.

4.2.2. Path in the External View

In the external view, the path is visualized as a tubular cutting geometry through the volume of the head. If the path is moved in another view, the virtual path will be updated automatically. This path offers the possibility of exploring the exact thickness and direction of the surgery access. If there are functional data, such as fiber tracts or activation regions along this path, the neurosurgeon can see them through the path and is able to modify the access direction. If there is no critical region visible, this path to the structure of interest may serve as an access route for the surgical intervention.

4.2.2.1. Computing the Path The cylindric path has a well defined geometric object that allows the identification of any voxels which are cut by the cylinder. The voxels that are located inside the cylinder will be discarded in the shader code (see Figure 5).

A cylinder is defined by its length and radius. The length $\boldsymbol{v}_{length}$ of the cylinder is the line from the incision point $\boldsymbol{p}_{incision}$ of the skull's surface to the center point $\boldsymbol{p}_{ROI}$ of the ROI. The incision point is marked by clicking onto the skull. The first hitpoint is retuned by tracing a ray through the volume. The radius c_{radius} is defined by the user. For every voxel, the distance to the intersection of the perpendicular line $\boldsymbol{p}_{cutpoint}$ with the center line of the cylinder is computed by solving the following equation:

$$\boldsymbol{p}_{cutpoint} = (((\boldsymbol{p}_{voxel} - \boldsymbol{p}_{ROI}) \cdot \hat{\boldsymbol{v}}_{length})\hat{\boldsymbol{v}}_{length}) + \boldsymbol{p}_{ROI}$$

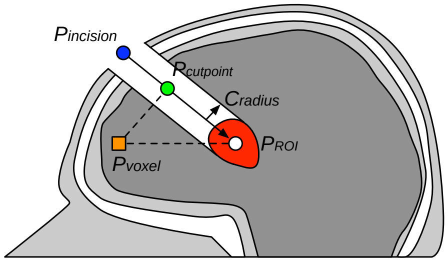

Figure 5: *Computation of the cylindric path from entry point to region of interest.*

In the fragment shader, all voxels $\boldsymbol{p}_{voxel}$ whose distance $d = ||\boldsymbol{p}_{voxel} - \boldsymbol{p}_{cut\,point}||$ to the cut point $\boldsymbol{p}_{cut\,point}$ is less than the radius of the cylinder c_{radius} will be discarded. Figure 6 and Figure 7 show the access path from the incision point to the ROI.

4.2.2.2. Visualization of the Path For a better three-dimensional perception and the enhancement of important landmarks in the external view, we have implemented lighting and boundary enhancement techniques. By using lighting and cutting planes, however, artifacts can appear in the volume. Since we use the gradient of the voxels for the lighting computation, we are not able to get correct results in homogenous regions of the volume where the gradients are ill defined. In order to cut a volume we have to transfer normals of the cutting geometry into the cutting surfaces of the volume (consistent shading [WEE03], see Figure 6).

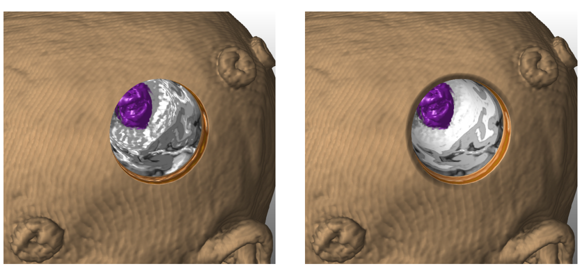

(a) (b)

Figure 6: *The cylindrical cut geometry without (a) and with consistent lighting (b). The visibility of anatomical details is superior with consistent shading.*

4.2.2.3. Additional Landmarks for Incision Point For neurosurgeons, landmarks at the skull as well as landmarks at the brain itself are particularly interesting. If the neurosurgeon opens the skull and removes pieces of the bone, the brain is visible. To accurately place the cut, landmarks of well-known brain structures are very important.

Therefore, we also add functionality to remove the skull interactively to visualize the anatomy of the brain. Since a volume mask of the brain is available, we are able to use per-tag-shading [LKP06] and to discard voxels of the skull. A shader program computes the distance between any voxel and the camera. By starting at a given distance threshold, voxels are discarded from the view (see Figure 7 (b)).

4.2.3. Path in MPR Views

In Section 3.2 we have discussed the additional integration of MPR views in our application. Since we display the virtual access path in the internal and external view, we extend the MPR views by adding a virtual cylinder. The cylinder allows the neurosurgeon to evaluate the path through the brain by slicing. Functional data such as activation areas and fibers are displayed altogether because attenuation is not required.

5. Results

We frequently discussed the proposed multimodal visualization techniques for neurosurgical therapy planning with three neurosurgeons and two neuro-radiologists, medical experts with substantial experience. The dual views allow to observe internal structures such as functional regions and lesions together with external structures and landmarks as the surface of skull and brain. Although we display the data in two different viewers, this concept has been well perceived by the medical experts because of the possibility of an initial observation of the functional data at minor interaction.

The distance based methods for attenuating anatomic details and for enhancing related functional structures enable the neurosurgeons to observe internal data without the need of slicing which was again received helpful. The coordinate system as well as the distance ring provide additional depth indicators. However, not all of the medical experts understood the distance ring intuitively. After illustrating its usage, the neurosurgeons deemed the distance ring very helpful for depth recognition particularly with regard to the standard medical views (axial, coronal, sagittal).

The detailed exploration was performed focussing on the opaque rendering of the external view. The neurosurgeons regarded the virtual access path as the major feature for surgery planning because of the possibility to find the trajectory to the lesion with respect to risk structures. For the medical experts the verification and fine-tuning of the virtual incision point was easy to achieve. Also, the visualization of the gyri and sulci as well as the skull's anatomy helps to recognize landmarks which let the access path transfer into the operation site. In particular cases, the MPR views helped the neurosurgeons to examine details of risk structures along the access path. The neurosurgeons tested our prototype and emphasized the high importance of multimodal volume rendering for neurosurgical therapy planning because it enables them to see risk structures extracted from different modalities along the virtual trajectory, e.g. fiber tracts combined with anatomical structures as lesion and brain tissue.

5.1. Implementation

We implemented the previously discussed methods with the rapid prototyping system *MeVisLab* using the OpenShading Language (GLSL) and image-processing modules. Our visualization prototype has been developed as an extension of an existing software platform for neurosurgical planning and monitoring where the raw image data are loaded and the preprocessing is performed. The segmentation of the brain was created by a semi-automatic watershed transformation, the data sets were aligned using inter-sequence co-registration. The resulting multimodal data are directly read into our prototype where the visualization is performed using a slice-based direct volume renderer. The data sets are loaded into the GPU memory and fused with blending functions.

5.2. Performance

All our methods achieve interactive frame rates. Figure 8 shows the average frame rates of the internal and external view (both 512x512 pixel) by performing a 360 degree rotation on a Mac Pro 2.66 GHz with 4 GB RAM and an ATI Radeon X1900 graphics card. The size of the MRT data set is 256x256x162 pixel and the size of the fMRI data set is 36x48x20 pixel.

6. Conclusions

This paper presents methods for visualizing multimodal volume data for neurosurgical tumor treatment which make use of modern graphics accelerators to allow interactive frame rates. The suggested methods for visualization allow the neurosurgeon to improve the neurosurgical planning. We believe the virtual access path could become an integral part of preoperative planning and promises to impact therapeutic decisions in neurosurgery.

Acknowledgments

The authors wish to thank Horst Hahn, Alexander Köhn, Florian Weiler, Dr. med. H.-H. Görge and Dr. med. Stephan Felber. Data used in this article are courtesy of Invivo Diagnostic Imaging, FL, and Lahey Clinic Burlington, MA.

References

[BBP*05] BLAAS J., BOTHA C. P., PETERS B., VOS F. M., POST F. H.: Fast and reproducible fiber bundle selection in DTI visualization. In *Proc. of IEEE Visualization* (2005), pp. 59–64.

[BG05] BRUCKNER S., GRÖLLER M. E.: VolumeShop: An Interactive System for Direct Volume Illustration. In *Proc. of IEEE Visualization* (2005).

[BGK06] BRUCKNER S., GRIMM S., KANITSAR A.: Illustrative Context-Preserving Exploration of Volume Data. *IEEE Trans. on Visualization and Computer Graphics 12*, 6 (2006), 1559–1569.

[BHWB07] BEYER J., HADWIGER M., WOLFSBERGER S., BÜHLER K.: High-Quality Multimodal Volume Rendering for Preoperative Planning of Neurosurgical Interventions. *IEEE Trans. Vis. Comput. Graph. 13*, 6 (2007), 1696–1703.

[CMH*01] CSÉBFALVI B., MROZ L., HAUSER H., KÖNIG A., GRÖLLER E.: Fast Visualization of Object Contours by Non-Photorealistic Volume Rendering. *Computer Graphics Forum 20*, 3 (2001).

[ER00] EBERT D., RHEINGANS P.: Volume illustration: non-photorealistic rendering of volume models. In *Proc. of IEEE Visualization* (2000), pp. 195–202.

[KKH02] KNISS J., KINDLMANN G., HANSEN C.: Multi-Dimensional Transfer Functions for Interactive Volume Rendering. *IEEE Trans. on Visualization and Computer Graphics 8*, 3 (2002), 270–285.

[KWK*07] KÖHN A., WEILER F., KLEIN J., KONRAD O., HAHN H. K., PEITGEN H.-O.: State-of-the-Art Computer Graphics in Neurosurgical Planning and Risk Assessment. In *Proc. of Eurographics Short Papers and Medical Prize Awards* (2007), pp. 117–120.

[LKP06] LINK F., KOENIG M., PEITGEN H.-O.: Multi-Resolution Volume Rendering with per Object Shading. In *Proc. of VMV* (2006), pp. 185–191.

[MFOF02] MANSSOUR I. H., FURUIE S. S., OLABARRIAGA S. D., FREITAS C. M. D. S.: Visualizing Inner Structures in Multimodal Volume Data. In *Proc. of IEEE SIBGRAPI* (2002), pp. 51–58.

[OW07] O'DONNELL L. J., WESTIN C.-F.: Automatic Tractography Segmentation Using a High-Dimensional White Matter Atlas. In *IEEE Trans. On Medical Imaging* (2007).

[RSK06] REZK-SALAMA C., KOLB A.: Opacity peeling for direct volume rendering. In *Computer Graphics Forum* (2006), vol. 25(3), pp. 597–606.

[RTF*06] RÖSSLER F., TEJADA E., FANGMEIER T., ERTL T., KNAUFF M.: GPU-based Multi-Volume Rendering for the Visualization of Functional Brain Images. In *Proc. of SimVis* (2006), pp. 305–318.

[SES05] SVAKHINE N., EBERT D. S., STREDNEY D.: Illustration Motifs for Effective Medical Volume Illustration. *IEEE Comput. Graph. Appl. 25*, 3 (2005), 31–39.

[TPD06] TAPPENBECK A., PREIM B., DICKEN V.: Distance-Based Transfer Function Design: Specification Methods and Applications. In *Simulation und Visualisierung* (2006), pp. 259–274.

[VFSG06] VIOLA I., FEIXAS M., SBERT M., GRÖLLER M. E.: Importance-Driven Focus of Attention. In *IEEE Trans. on Visualization and Computer Graphics* (2006).

[VZKL05] VILANOVA A., ZHANG S., KINDLMANN G., LAIDLAW D. H.: An Introduction to Visualization of Diffusion Tensor Imaging and its Applications. In *Visualization and Image Processing of Tensor Fields*. Springer-Verlag, 2005, pp. 121–153.

[WEE03] WEISKOPF D., ENGEL K., ERTL T.: Interactive Clipping Techniques for Texture-Based Volume Visualization and Volume Shading. *IEEE Trans. on Visualization and Computer Graphics* (2003), 298–312.

[WLM02] WILSON B., LUM E. B., MA K.-L.: Interactive Multi-volume Visualization. In *Proceedings of ICCS* (2002), pp. 102–110.

[ZDT04] ZHOU J., DÖRING A., TÖNNIES K. D.: Distance based enhancement for focal region based volume rendering. In *BVM* (2004), pp. 199–203.

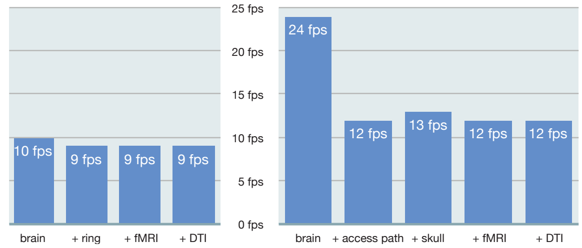

Figure 8: *Average frame rates of the internal view (left) and external view (right), with additional rendering features from left to right, respectively. The computation of the access path reduces performance by a factor of two. All other methods have negligible influence on the rendering performance.*

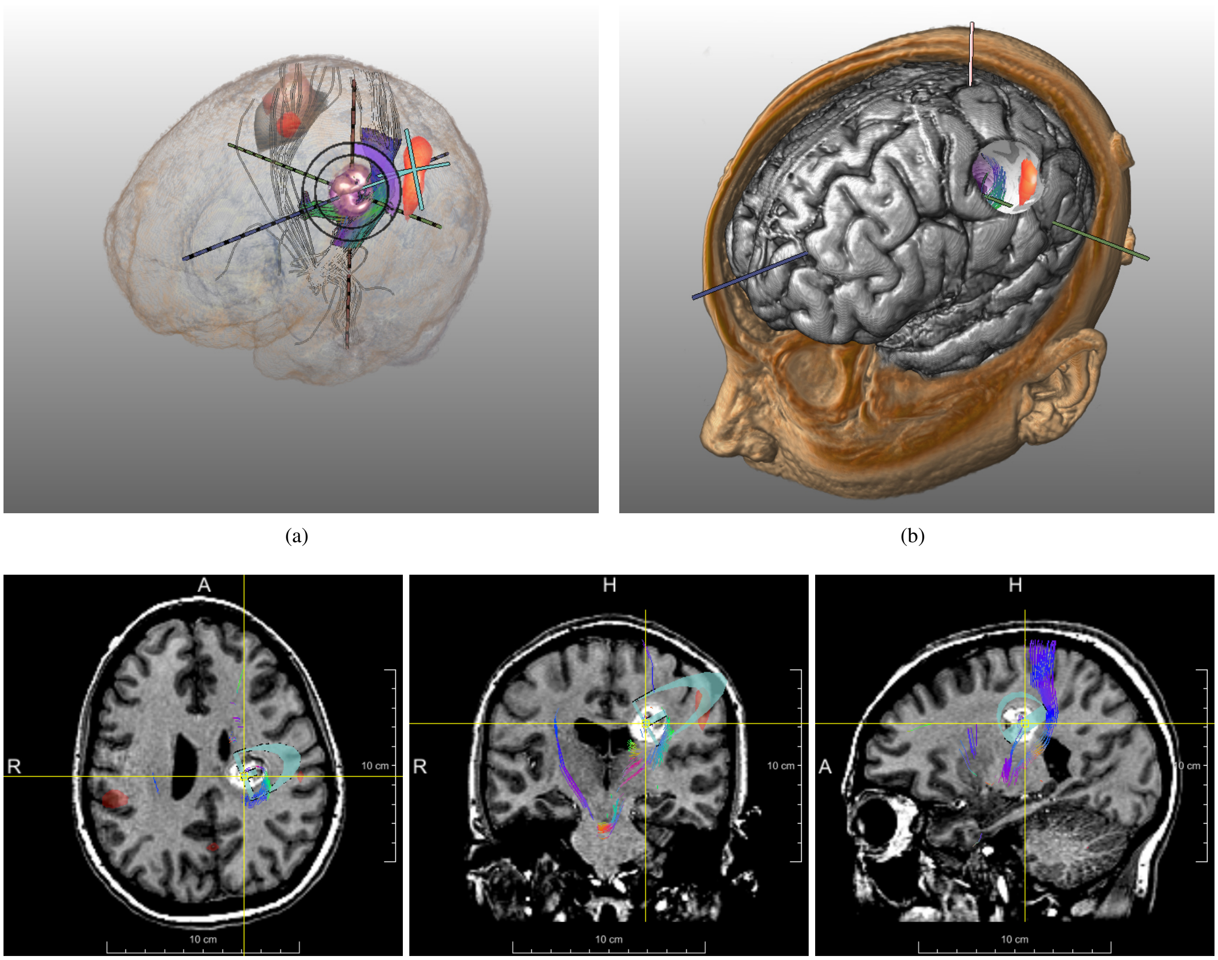

(a) (b)

(c) (d) (e)

Figure 7: *The three implemented views. In (a) the internal view shows the functional data and the presented techniques for enhancing the perception of the spatial depth. Figure (b) displays the corresponding external view with synchronized perspective. Each MPR view (c-e) shows a slice of the volume data, the virtual access path and functional as well as anatomical data.*